Critical current densities in ultrathin $Ba(Fe,Co)_2As_2$ microbridges

D. Rall,[1,2,*] K. Il'in,[2] K. Iida,[3] S. Haindl,[3] F. Kurth,[3] T. Thersleff,[3] L. Schultz,[3] B. Holzapfel,[3] and M. Siegel[2]

[1]*Lichttechnisches Institut (LTI), Karlsruher Institut für Technologie, Engesserstrasse 13, D-76131 Karlsruhe, Germany*

[2]*Institut für Mikro- und Nanoelektronische Systeme (IMS), Karlsruher Institut für Technologie, Hertzstrasse 16, D-76187 Karlsruhe, Germany*

[3]*Institute for Metallic Materials (IMW), IFW Dresden, P.O. Box 270116, D-01171 Dresden, Germany*

(Received 8 December 2010; published 18 April 2011)

The critical current density, j_C, in $Ba(Fe,Co)_2As_2$ thin-film microbridges was evaluated from current-voltage characteristics measured using a standard four-probe technique. The 90-nm-thick films were deposited by pulsed laser deposition on heated $(La,Sr)(Al,Ta)O_3$ substrates and patterned by means of photolithography and ion-milling techniques. The resulting microbridges show a good long-term stability and only minor degradation of the superconducting properties with respect to as-deposited films. The self-field j_C at $T = 4.2$ K reaches a value of about 3 MA/cm^2. The temperature dependence of j_C is described by $(1 - T/T_C)^{1.5}$, which is identical to the Ginzburg-Landau theory for the depairing critical current, in the wide temperature range $0.4 < T/T_C < 1$. Expulsion of the magnetic vortices is considered to be the mechanism responsible for overcoming Likharev's limit, where the width of the microbridge must be smaller than $4.4\xi_{GL}(T)$ to observe the depairing critical current.

DOI: 10.1103/PhysRevB.83.134514 PACS number(s): 74.25.Sv, 74.25.F−, 74.70.Xa, 74.78.−w

I. INTRODUCTION

Superconducting thin films offer a unique opportunity to study mesoscopic phenomena arising from a reduction in dimensionality since quasi-two-dimensional or even quasi-one-dimensional experimental situations can be achieved by thin-film structures with decreasing thickness. Low dimensionality becomes crucial whenever the geometrical size of the studied structure is comparable or even smaller than the characteristic lengths, such as the magnetic-field penetration depth, λ, and the coherence length, ξ. In addition, mesoscopic effects introduce a powerful way to tailor the wide variety of superconducting thin-film applications in the field of cryogenic quantum electronics.

The recent discovery of the iron-based superconductors[1] provides a new set of challenges for the field of superconducting thin-film growth, as researchers seek to understand the fundamental properties of this system as well as assess the suitability of these materials for the development of devices and applications. One of the iron-based superconducting families discovered to date[2,3] is $BaFe_2As_2$, which was dubbed the 122-family. Bulk samples with hole-doping $[(Ba_{1-x}K_x)Fe_2As_2]$ show superconducting transition temperatures of up to $T_C \approx 38$ K,[2] with electron doping $[Ba(Fe_{1-x}Co_x)_2As_2]$ up to 22 K.[4] As all iron-based superconductors, the 122-family also possesses the Fe*Pn* tetrahedron within its layer, where *Pn* is pnicogen or chalcogen. For general application purposes, the 122-family seems to be the most suitable among the iron-based superconductors because of their rather high critical temperature and upper critical field $B_{C2} \geqslant 45$ T,[5] low electronic anisotropy, reduced thermal fluctuations, and an apparently strong pinning of magnetic vortices.[6] Additionally, preparations of thin films made from the 122-family are easier than those from the F-doped LnFeAsO compounds (Ln being a rare-earth element). Furthermore, Ba-122 is more stable against exposure to moisture than Sr-122.[7]

Concerning devices, one of the crucial parameters of superconducting thin films is the critical current density, j_C, which determines the current-carrying ability of the final device fabricated from these films. There are two main mechanisms for the generation of the critical state caused by an applied transport current across a microbridge. The first mechanism is the depairing of Cooper pairs. This mechanism determines the ultimate limit of j_C. The second mechanism is typical for thin films made from type-II superconductors in which magnetic vortices penetrate into the thin films. In this case, the critical current is determined by competition between the pinning force attracting the vortex to a pinning site (e.g., defects of the crystalline microstructure of thin film) and the Lorentz force acting on this vortex in the presence of the externally applied transport current. Typical operation conditions of superconducting thin-film devices exclude externally applied magnetic fields or even special efforts are undertaken for absolute shielding of the devices against any sources of magnetic fields, including the Earth's magnetic field. Therefore, in low- as well as in high-T_C superconducting devices, one has to deal only with depinning of so called self-generated magnetic vortices, the vortices caused by penetration of the magnetic field generated by the applied transport current. According to Likharev,[8] magnetic vortices do not penetrate into superconducting bridges with a width W smaller than $4.4\xi_{GL}(T)$, where $\xi_{GL}(T)$ is the temperature-dependent Ginzburg-Landau coherence length. At temperatures in the vicinity of T_C, the coherence length diverges, thus realizing conditions for the observation of the depairing critical current. At low temperatures, where the condition $W < 4.4\xi_{GL}(T)$ is not satisfied anymore, penetration, depinning, and movement of magnetic vortices can significantly reduce j_C.

A number of experimental studies on the behavior of critical currents in the iron-based superconductors—particularly in $Ba(Fe,Co)_2As_2$ thin films and single crystals—have been conducted.[9] Numerous techniques have been applied for this. First, nondestructive measurements of the magnetization allow one to estimate the critical current density on the basis of Bean's critical state model.[10,11] Second, magneto-optical imaging can be used to study the structure of the critical state by analyzing the spatial distribution of the magnetic induction on the sample.[12] Third, the study of the time-dependent

magnetization as a function of temperature and magnetic field enables the estimation of the critical current density determined by the creep of magnetic flux. All the above-mentioned magnetic techniques are noninvasive, i.e., they can be performed on nonpatterned films and single crystals. However, the presence of an applied magnetic field creates an experimental situation significantly different from the one realized in the transport measurements. Here, the critical state is generated by an applied current in the absence of any external magnetic fields. In thick films and bulk samples, the critical current can reach very high values due to a large cross section, which makes it more difficult to achieve reliable transport current measurements. Therefore, patterning of thin films into micrometer-sized structures is required, thus making transport experiments more reliable for any estimation of application potential of superconducting thin films.

The critical current density in $Ba(Fe,Co)_2As_2$ evaluated by magnetization measurements in single crystals is found to be $(3–4)\times10^5$ A/cm^2 at 4.2 K.[13,14] Early results obtained on thin films were typically below 10^5 A/cm^2.[15] However, a j_C value of 4×10^6 A/cm^2 has been recently reported for a 250-nm-thick epitaxial $Ba(Fe,Co)_2As_2$ film on $(La,Sr)(Al,Ta)O_3$ (LSAT) (001) substrate,[16] and similar values are found in $Fe/Ba(Fe,Co)_2As_2$ bilayers.[17] Comparable j_C values were reported for composite films including correlated defects, which may enhance pinning.[18,19] In spite of numerous works reporting on temperature and magnetic-field dependence of j_C in single crystal and thin films, there is a lack of experiments performed on patterned films, i.e., on microbridges made from $Ba(Fe,Co)_2As_2$ films.

In this paper, we present transport properties of microbridges made from a 90-nm-thick $Ba(Fe,Co)_2As_2$ film. Details on the fabrication of thin films and their patterning into microbridges are given in Sec. II. In Sec. III, we present results on direct measurements of normal-state and superconducting properties of the fabricated microbridges. The temperature dependencies of the critical current density extracted from the current-voltage characteristics and their analysis based of the Ginzburg-Landau theory for the depairing critical current are given in Sec. IV.

II. EXPERIMENTAL

The investigated $Ba(Fe,Co)_2As_2$ film was grown by pulsed laser deposition (PLD) on an LSAT (100) substrate kept at 650 °C during deposition. The deposition was made under ultrahigh-vacuum condition with a base pressure of 10^{-9} mbar in the process chamber. The nominal target composition is $Ba(Fe_{0.9}Co_{0.1})_2As_2$. Stoichiometric transfer from the target to the film during the PLD process was confirmed by Rutherford backscattering. The film was confirmed to be *c*-axis-textured by x-ray diffraction (XRD) in Bragg-Brentano geometry with Co $K\alpha$ radiation. The detailed film preparation can be found in Ref. 20. The microstructure of the film was investigated on a C_s-corrected FEI Titan^3 transmission electron microscope (TEM) operating at 300 kV. The TEM lamella was prepared on a Carl Zeiss 1540 XB focused ion beam using the *in situ* lift-out method. The TEM investigation confirms the film thickness, d, as being 90 nm and can rule out the presence of secondary phases or rotated grains in the Ba-122 film (see Fig. 1). However, a 2-nm-thick reaction layer at the interface is observed. Spectroscopy measurements indicate that this layer is iron-rich and barium-poor. It may represent an epitaxial iron layer, similar to the results in Ref. 15. Iron is known to form a highly stable bond with Ba-122 (Ref. 21), and this may be responsible for the presence of an Fe (002) peak in the Bragg-Brentano XRD data. However, the TEM investigation on this sample revealed no biaxially textured iron at this interface. Instead, considerable amounts of what appears to be iron oxide were observed. It is possible that this is a consequence of the TEM lamella preparation and storage, although this is currently under further investigation.

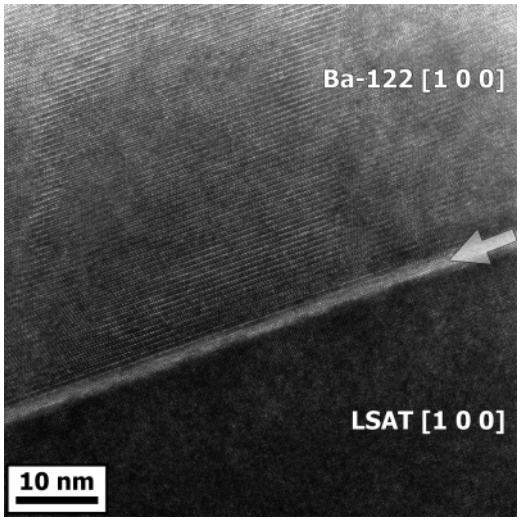

FIG. 1. TEM image of the $Ba(Fe,Co)_2As_2$ film on an LSAT substrate. A thin iron-rich interfacial layer (indicated by arrow) forms at the film-substrate boundary.

The film has been patterned into single bridges with equal length $L = 50$ μm and different width $1 < W < 10$ μm connected to mm^2-sized contact pads. The patterning of the film was accomplished using standard photolithography and ion-milling techniques. During the process, the $Ba(Fe,Co)_2As_2$ structures were protected by a photoresist layer remaining on top of the bridges after exposure and development of the resist and thus were not in direct contact with the AZ-developer and water used as a stopper. The thickness of the photoresist ($\approx$1.2 μm) was large enough to prevent damaging of the film under the resist during the etching process performed by bombardment of Ar ions accelerated in an electrical field of $U = 250$ V. Therefore, we assumed that this procedure should not detrimentally influence the transport properties of the $Ba(Fe,Co)_2As_2$ thin-film structures, as was subsequently confirmed by measurements of superconducting and normal-state properties of micrometer-wide bridges made from this film. After patterning, the remaining photoresist was removed from the surface of the bridges in an acetone bath and then cleaned with isopropanol. The electrical contact was established by manually attached indium wire bonds to the contact pads (two current leads and two voltage contacts) of each structure. The actual width of the microbridges was confirmed with a scanning electron microscope (SEM).

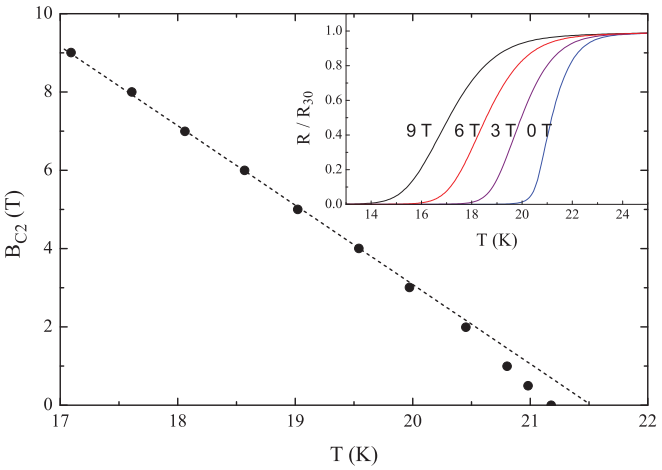

FIG. 2. (Color online) Temperature dependence of the second critical magnetic field (taken at $0.5R_{30}$), measured at unpatterned films. The dashed line shows a linear fit of the low-temperature part of the $B_{C2}(T)$ curve. The inset shows the temperature dependence of the normalized resistance for different magnetic fields as indicated in the graph.

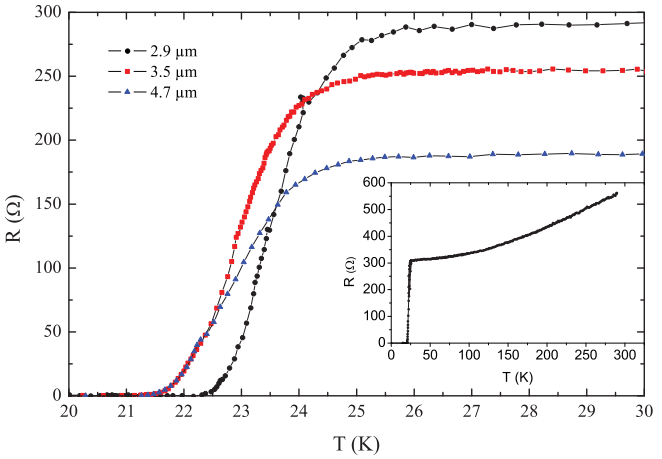

FIG. 3. (Color online) The temperature dependence of the resistance in the vicinity of the superconducting transition of three bridges with different widths as indicated in the legend. The inset shows the $R(T)$ curve in the whole temperature range for the 2.9-μm-wide bridge.

III. RESULTS

The T_C value of the transition onset of the $Ba(Fe,Co)_2As_2$ film before patterning was ≈23 K, which was measured by a standard four-probe technique in a commercial PPMS (physical property measurement system). Series of $R(T)$ curves have been measured at different magnetic field up to 9 T applied normal to the surface of the film (see the inset in Fig. 2). We have observed a broadening of the resistive transition with increasing applied magnetic fields. The transition width $\Delta T = T(0.9R_{30}) - T(0.1R_{30})$ (R_{30} is the resistance of a microbridge in the normal state at $T = 30$ K, i.e., well above the superconducting transition) increases from about 1.8 K at zero magnetic field to almost 4 K at 9 T and may be explained by inhomogeneities of the film. The temperature dependence of the upper critical field, B_{C2}, taken at $0.5R_{30}$ is linear at low temperatures (approximately below $0.9T_C$) with $dB_{C2}/dT = -2.06$ T/K. A slight deviation from linearity close to T_C is observed.

The temperature dependencies of resistance of all fabricated bridges were measured in a standard four-probe experimental setup in a liquid-helium transport dewar in the temperature range from 4.2 K up to room temperature $T = 295$ K (Fig. 3). During the $R(T)$ measurements, the bridges were biased with a constant current of less than 1 μA applied from the low noise current source. The applied current was small enough to avoid overheating of the measured samples. The T_C was defined as the temperature at which resistance of a bridge becomes smaller than $0.01R_{30}$. The R-T curves show a decrease of the resistance with decreasing temperature (see the inset in Fig. 3) typical for $Ba(Fe,Co)_2As_2$ films, followed by the superconducting transition with $T_C \approx 22$ K. Therefore, the processing results only in a minor decrease of the T_C with respect to nonpatterned film. The ratio of the resistance at 295 K to R_{30} was found to be $R_{295}/R_{30} \approx 1.9$. The width of the superconducting transition of all bridges, $\Delta T \approx 2$ K, is almost the same ΔT value as of nonpatterned film at zero magnetic fields (see the inset in Fig. 2) that additionally confirms the stability of the film against the fabrication process. From the resistance of the bridges measured at $T = 30$ K and their geometry, the residual resistivity was estimated to be $\rho_{30} \approx 155$ $\mu\Omega$ cm, which is about two to three times smaller than what was reported previously.[5,16,22] Multiple measurements of the microbridges were made within a few months after patterning. Although the microbridges were thermocycled at least six times at different conditions (i.e., in He gas and in vacuum), both T_C and j_C at 4.2 K always showed the same values within the measurement accuracy, demonstrating good long-term as well as thermal stability.

The current-voltage characteristics (I-V curves) were measured in the current-bias mode in the same experimental setup (Fig. 4). At temperatures $T < 0.85T_C$, the I-V curves are hysteretic and show a sharp jump of the microbridges from superconducting to normal state. The current at which this jump is observed defines the critical current at the given

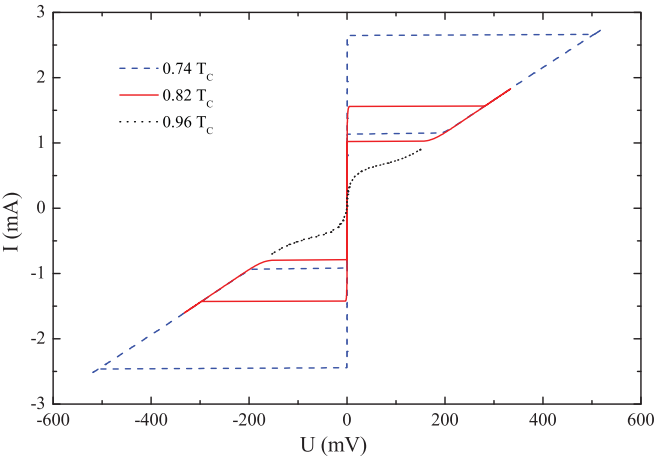

FIG. 4. (Color online) Current-voltage characteristics of the bridge with width $W = 4.7$ μm measured at different temperatures as indicated in the legend.

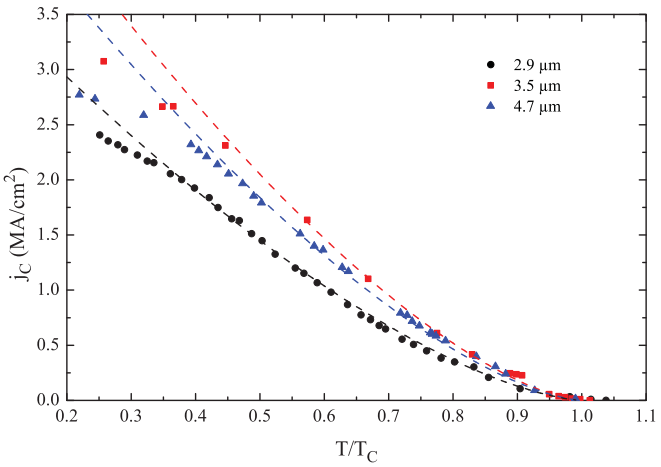

FIG. 5. (Color online) Temperature dependencies of the critical current density of three studied bridges (symbols). The dashed lines are the theoretical fits by Eq. (1) and coincide well with the measurements down to $T/T_C \approx 0.4$. The widths of the bridges are indicated in the legend.

temperature, $I_C(T)$. The hysteresis current (the current at which the bridge returns into the superconducting state with the decrease in applied current) is determined by equilibrium between the Joule heating power dissipated in a microbridge and the efficiency of thermal flow through the film-substrate interface. At temperatures in the vicinity of T_C, the *I-V* curves show a smooth transition from the superconducting to the resistive and then to the normal state of the microbridge. In this case, the critical current was determined as the current at which the voltage deviates from zero by 100 μV. This criterion is limited by the resolution of our measurement system and corresponds to a resistance of about 1 Ω, which is <1% of the resistance in the normal state above the transition for all studied microbridges.

The resulting dependences of $j_C = I_C/(Wd)$ on reduced temperature $t = T/T_C$ are shown in Fig. 5 for three bridges with different width. At $T = 4.2$ K, j_C reaches values of $\approx 2.8 \pm 0.4$ MA/cm^2, which is significantly higher than the value reported for single crystals[13,14] and comparable to recently reported values of 4 MA/cm^2 measured in a 250-nm-thick Co-doped $Ba(Fe,Co)_2As_2$ epitaxial film[16] or obtained in Fe/$Ba(Fe,Co)_2As_2$ bilayers.[17] The observed spread in j_C values between microbridges may be caused by spatial nonuniformity of the film properties.

IV. DISCUSSION

Before we analyze the obtained results on the temperature dependence of j_C, we recall the mechanisms of critical state formation and conditions for their predominance in microbridges biased with a transport current and without an externally applied magnetic field. The ultimate value of the j_C is determined by the Cooper pair breaking mechanism. In the case of microbridges with a width smaller than $4.4\xi_{GL}(T)$, the j_C can be determined by this mechanism solely due to full prevention of magnetic vortex penetration into a microbridge. In microbridges wider than $4.4\xi_{GL}(T)$, there is a space for nucleation of the magnetic vortices that may significantly reduce the critical current. The presence of magnetic vortices with a normal core of about $2\xi_{GL}(T)$ effectively reduces the width of the microbridge available to carry a supercurrent. In spite of the presence of magnetic vortices in the bridge, the critical current can still be determined by the depairing of the Cooper pairs in the case of strong pinning, although the measured critical current will be smaller than the one expected from the superconducting properties and the geometry of the microbridge. Moreover, if the Lorentz force acting on vortices in the presence of a transport current exceeds the pinning force, the depinning and the movement of magnetic vortices results in energy dissipation and thus the microbridge transfers from the superconducting to the resistive state. In the case of weak pinning, the critical current determined by the vortex depinning mechanism can be much smaller than the depairing critical current.

The upper critical field for our $Ba(Fe,Co)_2As_2$ films estimated in the Werthamer-Helfand-Hohenberg limit[23] $B_{C2}(0) = -0.69 T_C dB_{C2}/dT$ is 31 T, and the corresponding value of the Ginzburg-Landau coherence length at zero temperature, $\xi_{GL}(0)$, is about 3.3 nm. Since the coherence length and even $4.4\xi_{GL}(0)$ are much smaller than the width of all our microbridges, there are no strong inhibitions for the penetration of magnetic vortices into microbridges. Due to its temperature dependence, the coherence length diverges at $T \to T_C$, the condition $W < 4.4\xi_{GL}$ can be satisfied, and the critical current measured in this temperature range will be determined by the depairing mechanism of the critical state. For the narrowest bridge with $W = 2.9$ μm, this criterion limits the temperature range for the full vortex expulsion to $T > 0.997T_C$. To find the value of the ultimate current density for our $Ba(Fe,Co)_2As_2$ films, we fit $j_C(t)$ by employing the Ginzburg-Landau theory for the depairing critical current,

$$j_C^{GL}(t) = j_C^{GL}(0)\,[1-t]^{\frac{3}{2}}, \tag{1}$$

shown by dashed lines in Fig. 5. The $j_C^{GL}(0)$ is the depairing critical current density at zero temperature,

$$j_C^{GL}(0) = 1.932\frac{\Delta(0)^{\frac{3}{2}}}{e\rho_{30}\sqrt{D\hbar}}, \tag{2}$$

where $\hbar$ is the Planck constant, $\Delta(0)$ is the superconducting energy gap at 0 K, ρ_{30} is the residual resistivity, e is the electron charge, and D is the electron diffusion coefficient,

$$D = -\frac{4k_B}{\pi e}\left[\frac{dB_{C2}}{dT}\right]^{-1}_{T=T_C}, \tag{3}$$

with k_B the Boltzmann constant.

Contrary to the estimated very narrow temperature interval, we observed surprisingly that the experimental $j_C(t)$ dependence for this bridge follows the Ginzburg-Landau theoretical predictions Eq. (1) in the much wider temperature range from the critical temperature down to about $t = 0.4$ (see Fig. 5). Only below $t = 0.4$ does the $j_C(t)$ curve deviate from theory significantly, demonstrating a change of conditions of the critical state generation. For wider bridges, the temperature dependence of j_C looks similar to that measured on the narrowest microbridge in perfect coincidence with theory [Eq. (1)] in a very wide temperature range down to about

$t = 0.45$–0.5 followed by deviation of experimental data toward values lower than predicted by theory at $t < 0.4$.

We assume that the decrease of j_C below the theoretical predictions at $t < 0.4$ relates to the penetration only or to the penetration and the movement of magnetic vortices. There are two requirements to be fulfilled in wide microbridges ($W < 4.4\xi_{GL}$) to make the mechanism of penetration and depinning of the magnetic vortex dominating over the depairing mechanism for the critical state generation:

(i) A source of magnetic field has to be strong enough to overcome the potential barrier for vortex penetration.

(ii) A transport current has to be strong enough to overcome the pinning potential.

One possible source for a magnetic field in our experiments (besides the Earth's magnetic field, which is too weak) is the transport current applied to the microbridge. The magnetic field created by the transport current with density j_{tr} at the edges of such a microbridge is

$$B_{edge} = \frac{\mu_0 j_{tr}\sqrt{Wd}}{2\pi}, \tag{4}$$

where μ_0 is the vacuum permeability. For the widest bridge with $W = 4.7$ μm and with the applied current close to the critical current value at 4.2 K, the B_{edge} is about 3.6 mT, i.e., four times lower than the first critical magnetic field $B_{C1}(4.2\ \text{K}) = 14$ mT estimated as

$$B_{C1}(t) = \frac{\Phi_0}{4\pi\lambda^2}\left[\ln\left(\frac{\lambda(t)}{\xi_{GL}(t)}\right) + 0.08\right], \tag{5}$$

where Φ_0 is the magnetic flux quantum and $\lambda(t)$ is the temperature-dependent magnetic-field penetration depth calculated in the dirty limit using only experimentally measured quantities

$$\lambda = \sqrt{\frac{\hbar\rho_{30}}{2\pi\mu_0 k_B T_C}}(1 - t^4)^{-\frac{1}{2}}. \tag{6}$$

Although B_{edge} is lower than B_{C1} at these temperatures, there is a probability for vortices to overcome the energy barrier and to penetrate into the microbridge. The height of the energy barrier for the vortex penetration is strongly dependent on the quality of the bridge edges. Different defects are caused by damaging of the edges by Ar ion bombardment during the etching process and may significantly reduce the barrier height locally. Therefore, a deviation of j_C from Eq. (1) at low temperatures may be due to the penetration of magnetic vortices and their movement under the influence of the Lorentz force.

The "surprisingly broad" temperature range [wider than expected from the $W < 4.4\xi_{GL}(T)$ criteria] of the depairing critical current observation has been experimentally demonstrated recently in Nb thin-film bridges with a width of a few hundred nanometers.[24] However, there are a few significant features that make the situation with the studied $Ba(Fe,Co)_2As_2$ thin-film microbridges quite interesting. First, we have to note the much wider temperature range of the coincidence of the experimentally measured $j_C(t)$ with the predictions of the Ginzburg-Landau theory [Eq. (1)]. In the case of the Nb thin-film bridges, this temperature interval was limited by the minimum relative temperature $t \approx 0.7$ (see Fig. 3 in Ref. 24). In the studied $Ba(Fe,Co)_2As_2$ microbridges, the minimum temperature is $t \approx 0.4$, i.e., the temperature range of the coincidence is almost two times larger in relative units of t and six times wider in the absolute temperature units [12 and 2 K for $Ba(Fe,Co)_2As_2$ and Nb bridges, respectively]. The second difference is the bridge width, for which the temperature dependence of j_C caused by the depairing mechanism has been observed. The micrometer-wide Nb bridges showed a deviation from the depairing theory at temperatures much higher than $0.7T_C$, and only in the submicrometer-wide bridges ($W \leqslant 0.5$ μm) did the temperature range of coincidence reach the maximum. The widest $Ba(Fe,Co)_2As_2$ thin-film bridge has a width of about one order of magnitude larger ($W = 4.7$ μm) and shows a deviation from theory only at $t < 0.45$.

The strong difference between Nb and $Ba(Fe,Co)_2As_2$ thin-film bridges in the temperature range of coincidence of $j_C(t)$ with theory, as well as in the "required" bridge width, in which this coincidence is observed, can be understood to account for the almost one order of magnitude smaller value of the critical current density measured in $Ba(Fe,Co)_2As_2$ thin-film bridges compared to the Nb bridges at the same relative temperature. Since B_{C1} [see Eq. (5)] in both materials is similar, 22 and 33 mT in Nb and $Ba(Fe,Co)_2As_2$, respectively, the magnetic field created by the smaller applied current density does not allow us to overcome the penetration barrier for vortices even in relatively wide, micrometer-sized $Ba(Fe,Co)_2As_2$ bridges.

The value of the j_C estimated for our $Ba(Fe,Co)_2As_2$ thin films using Eq. (2) and experimentally measured parameters is about 46.5 MA/cm^2 at $T = 0$ K and 21.6 MA/cm^2 at $T = 4.2$ K. The value of $\Delta(0) = 1.05k_BT_C$ (used for these calculations) has been found for similar films using the temperature-dependent optical reflectivity and complex transmissivity measured in a wide spectra range from THz up to ultraviolet.[25] The calculated values of the deparing critical current density are about eight times larger than the experimentally measured $j_C(4.2\ \text{K}) = 2.8 \pm 0.4$ MA/cm^2 and the values obtained by extrapolation of the theoretical fit of Eq. (1) to zero temperature. The difference between calculated and measured j_C values, and the spread of j_C among the bridges, can be caused by a nonuniformity of the effective superconducting cross section of the bridge, which can be smaller than what is defined by the measured width (SEM) and thickness (TEM). The exact reasons for this nonuniformity and for the reduction of the effective cross section are still unclear and require additional more systematic studies of the transport and microstructure properties of thin pnictide films.

V. CONCLUSION

Transport properties of micrometer-sized bridges made by photolithography and ion milling from the 90-nm-thick $Ba(Fe,Co)_2As_2$ film grown on an LSAT substrate by the PLD technique were resistively measured. The temperature dependence of the critical current density measured without externally applied magnetic field is well described by the Ginzburg-Landau theory in the very wide interval of the reduced temperature $0.4 < t < 1$. In spite of the fact that

the bridges are much wider than the coherence length, the critical current in thin $Ba(Fe,Co)_2As_2$ film microbridges is determined by the Cooper pair breaking mechanism since the self-generated magnetic field is not strong enough to exceed the barrier for penetration of magnetic vortices into the microbridge. The critical current density of the $Ba(Fe,Co)_2As_2$ microbridges has been measured up to values $j_C(4.2\ \mathrm{K}) \approx 3.1\ \mathrm{MA/cm^2}$.

ACKNOWLEDGMENTS

The authors from IFW Dresden would like to acknowledge technical support by Juliane Scheiter and financial support from the German Research Foundation under project HA 5934/3-1. D.R. is thankful to Karlsruhe School of Optics and Photonics for financial support. This work is also supported in part by Karlsruhe DFG Center for Functional Nanostructures.

*dagmar.rall@student.kit.edu

[1] Y. Kamihara, T. Watanabe, M. Hirano, and H. Hosono, J. Am. Chem. Soc. **130**, 3296 (2008).

[2] M. Rotter, M. Tegel, and D. Johrendt, Phys. Rev. Lett. **101**, 107006 (2008).

[3] F. C. Hsu, J. Y. Luo, K. W. Yeh, T. K. Chen, T. W. Huang, P. Wu, Y. C. Lee, Y. L. Huang, Y. Y. Chu, D. C. Yan, and M. K. Wu, Proc. Natl. Acad. Sci. USA **105**, 14262 (2008).

[4] A. S. Sefat, R. Jin, M. A. McGuire, B. C. Sales, D. J. Singh, and D. Mandrus, Phys. Rev. Lett. **101**, 117004 (2008).

[5] S. A. Baily, Y. Kohama, H. Hiramatsu, B. Maiorov, F. F. Balakirev, M. Hirano, and H. Hosono, Phys. Rev. Lett. **102**, 117004 (2009).

[6] M. Putti, I. Pallecchi, E. Bellingeri, M. R. Cimberle, M. Tropeano, C. Ferdeghini, A. Palenzona, C. Tarantini, A. Yamamoto, J. Jiang, J. Jaroszynski, F. Kametani, D. Abraimov, A. Polyanskii, J. D. Weiss, E. E. Hellstrom, A. Gurevich, D. C. Larbalestier, R. Jin, B. C. Sales, A. S. Sefat, M. A. McGuire, D. Mandrus, P. Cheng, Y. Jia, H. H. Wen, S. Lee, and C. B. Eom, Supercond. Sci. Technol. **23**, 034003 (2010).

[7] T. Katase, H. Hiramatsu, H. Yanagi, T. Kamiya, M. Hirano, and H. Hosono, Solid State Commun. **149**, 2121 (2009).

[8] K. K. Likharev, Rev. Mod. Phys. **51**, 101 (1979).

[9] L. Luan, O. M. Auslaender, T. M. Lippman, C. W. Hicks, B. Kalisky, J.-H. Chu, J. G. Analytis, I. R. Fisher, J. R. Kirtley, and K. A. Moler, Phys. Rev. B **81**, 100501 (2010).

[10] C. P. Bean, Phys. Rev. Lett. **8**, 250 (1962).

[11] C. P. Bean, Rev. Mod. Phys. **36**, 31 (1964).

[12] R. Prozorov, M. A. Tanatar, R. T. Gordon, C. Martin, H. Kim, V. G. Kogan, N. Ni, M. E. Tillman, S. L. Bud'ko, and P. C. Canfield, Physica C **469**, 582 (2009).

[13] A. Yamamoto, J. Jaroszynski, C. Tarantini, L. Balicas, J. Jiang, A. Gurevich, D. C. Larbalestier, R. Jin, A. S. Sefat, M. A. McCuire, B. C. Sales, D. K. Christen, and D. Mandrus, Appl. Phys. Lett. **94**, 062511 (2009).

[14] R. Prozorov, N. Ni, M. A. Tanatar, V. G. Kogan, R. T. Gordon, C. Martin, E. C. Blomberg, P. Prommapan, J. Q. Yan, S. L. Bud'ko, and P. C. Canfield, Phys. Rev. B **78**, 224506 (2008).

[15] K. Iida, J. Hänisch, T. Thersleff, F. Kurth, M. Kidszun, S. Haindl, R. Hühne, L. Schultz, and B. Holzapfel, Phys. Rev. B **81**, 100507 (2010).

[16] T. Katase, Y. Ishimaru, A. Tsukamoto, H. Hiramatsu, T. Kamiya, K. Tanabe, and H. Hosono, Appl. Phys. Lett. **96**, 142507 (2010).

[17] K. Iida, S. Haindl, T. Thersleff, J. Hänisch, F. Kurth, M. Kidszun, R. Hühne, I. Mönch, L. Schultz, B. Holzapfel, and R. Heller, Appl. Phys. Lett. **97**, 172507 (2010).

[18] C. Tarantini, S. Lee, Y. Zhang, J. Jiang, C. W. Bark, J. D. Weiss, A. Polanskii, C. T. Nelson, H. W. Jang, C. M. Folkman, S. H. Baek, X. Q. Pan, A. Gurevich, E. E. Hellstrom, C. B. Eom, and D. C. Larbalestier, Appl. Phys. Lett. **96**, 142510 (2010).

[19] S. Lee, J. Jiang, Y. Zhang, C. W. Bark, J. D. Weiss, C. Tarantini, C. T. Nelson, H. W. Jang, C. M. Folkman, S. H. Baek, A. Polyanskii, D. Abraimov, A. Yamamoto, J. W. Park, X. Q. Pan, E. E. Hellstrom, D. C. Larbalestier, and C. B. Eom, Nat. Mater. **9**, 397 (2010).

[20] K. Iida, J. Hänisch, R. Hühne, F. Kurth, M. Kidszun, S. Haindl, J. Werner, L. Schultz, and B. Holzapfel, Appl. Phys. Lett. **95**, 192501 (2009).

[21] T. Thersleff, K. Iida, S. Haindl, M. Kidszun, D. Pohl, A. Hartmann, F. Kurth, J. Hänisch, R. Hühne, B. Rellinghaus, L. Schultz, and B. Holzapfel, Appl. Phys. Lett. **97**, 022506 (2010).

[22] C. Tarantini, S. Lee, Y. Zhang, J. Jiang, C. W. Bark, J. D. Weiss, A. Polyanskii, C. T. Nelson, H. W. Jang, C. M. Folkman, S. H. Baek, X. Q. Pan, A. Gurevich, E. E. Hellstrom, C. B. Eom, and D. C. Larbalestier, Appl. Phys. Lett. **96**, 142510 (2010).

[23] N. R. Werthamer, E. Helfand, and P. C. Hohenberg, Phys. Rev. **147**, 295 (1966).

[24] K. Ilin, D. Rall, M. Siegel, A. Engel, A. Schilling, A. Semenov, and H.-W. Hübers, Physica C **470**, 953 (2010).

[25] B. Gorshunov, D. Wu, A. A. Voronkov, P. Kallina, K. Iida, S. Haindl, F. Kurth, L. Schultz, B. Holzapfel, and M. Dressel, Phys. Rev. B **81**, 060509 (2010).